






# Possible experimental realization of a basic $Z_2$ topological semimetal in GaGeTe

Cite as: APL Mater. **7**, 121106 (2019); <https://doi.org/10.1063/1.5124563>

Submitted: 15 August 2019 . Accepted: 22 November 2019 . Published Online: 12 December 2019

Erik Haubold, Alexander Fedorov, Florian Pielhofer , Igor P. Rusinov , Tatiana V. Menshchikova, Viola Duppel, Daniel Friedrich, Richard Weihrich, Arno Pfitzner , Alexander Zeugner, Anna Isaeva, Setti Thirupathaiah, Yevhen Kushnirenko, Emile Rienks, Timur Kim , Evgueni V. Chulkov, Bernd Büchner, and Sergey Borisenko 

## COLLECTIONS

Paper published as part of the special topic on [Topological Semimetals & New Directions](#)

Note: This paper is part of the Special Topic on Topological Semimetals—New Directions.



View Online



Export Citation



CrossMark

## ARTICLES YOU MAY BE INTERESTED IN

[Dirac fermions and possible weak antilocalization in LaCuSb<sub>2</sub>](#)


APL Materials **7**, 121108 (2019); <https://doi.org/10.1063/1.5124685>

[Superconducting order parameter of the nodal-line semimetal NaAlSi](#)

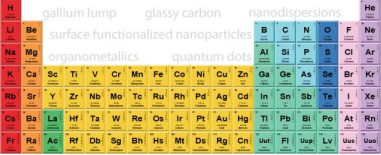
APL Materials **7**, 121103 (2019); <https://doi.org/10.1063/1.5124242>

[Weyl nodes and magnetostructural instability in antiperovskite Mn<sub>3</sub>ZnC](#)

APL Materials **7**, 121104 (2019); <https://doi.org/10.1063/1.5129689>



THE ADVANCED MATERIALS MANUFACTURER®



additive manufacturing   epitaxial crystal growth   cerium oxide polishing powder   silver nanoparticles   sputtering targets   III-IV semiconductors   CVD precursors   europium phosphors

deposition slugs   OLED lighting   spintronics   solar energy   osmium   nanoribbons   thin films   chalcogenides   AuNPs   GDC   Li-ion battery electrolytes   99.999% ruthenium spheres

endohedral fullerenes   copper nanoparticles   diamond micropowder   CIGS   MBE grade materials   palladium catalysts   flexible electronics   beta-barium borate   borosilicate glass   dysprosium pellets   YBCO   pyrolytic graphite   3d graphene foam   indium tin oxide   mesoporous silica   raman substrates   sapphire windows   tungsten carbide   InGaAs   barium fluoride   carbon nanotubes   lithium niobate   scandium powder

gallium lump   glassy carbon   nanodispersions   InAs wafers   laser crystals   ultra high purity materials   MOFs   rare earth metals   photovoltaics   refractory metals   MOCVD   superconductors   transparent ceramics   ultra high purity silicon

American Elements opens up a world of possibilities so you can **Now Invent!**

Over 15,000 certified high purity laboratory chemicals, metals, & advanced materials and a state-of-the-art Research Center. Printable GHS-compliant Safety Data Sheets. Thousands of new products. And much more. All on a secure multi-language "Mobile Responsive" platform.

perovskite crystals   yttrium iron garnet   alternative energy   h-BN   gold nanocubes   graphene oxide   macromolecules   photonics   rhodium sponge   fiber optics   beamsplitters   infrared dyes   zeolites   fused quartz   metallocenes   platinum ink   buckyballs   Ti-6Al-4V

**Now Invent.™**  
The Next Generation of Material Science Catalogs

[www.americanelements.com](http://www.americanelements.com)





# Possible experimental realization of a basic $Z_2$ topological semimetal in GaGeTe

Cite as: APL Mater. 7, 121106 (2019); doi: 10.1063/1.5124563

Submitted: 15 August 2019 • Accepted: 22 November 2019 •

Published Online: 12 December 2019



Erik Haubold,<sup>1,a)</sup> Alexander Fedorov,<sup>1,2</sup> Florian Pielhofer,<sup>3,4,b)</sup>  Igor P. Rusinov,<sup>5,6</sup>  Tatiana V. Menshchikova,<sup>5</sup> Viola Duppel,<sup>3</sup> Daniel Friedrich,<sup>4</sup> Richard Wehrich,<sup>7</sup> Arno Pfitzner,<sup>4</sup>  Alexander Zeugner,<sup>1,8</sup> Anna Isaeva,<sup>1,8</sup> Setti Thirupathiah,<sup>1,c)</sup> Yevhen Kushnirenko,<sup>1</sup> Emile Rienks,<sup>1,8</sup> Timur Kim,<sup>9</sup>  Evgueni V. Chulkov,<sup>5,6,10,11</sup> Bernd Büchner,<sup>1,8</sup> and Sergey Borisenko<sup>1,d)</sup> 

## AFFILIATIONS

<sup>1</sup> IFW Dresden, Helmholtzstr. 20, 01069 Dresden, Germany

<sup>2</sup> HZB Helmholtz-Zentrum Berlin für Materialien und Energie, Albert-Einstein-Str. 15, 12489 Berlin, Germany

<sup>3</sup> Max Planck Institute for Solid State Research, Heisenbergstr. 1, 70569 Stuttgart, Germany

<sup>4</sup> Institut für Anorganische Chemie, Universität Regensburg, 93040 Regensburg, Germany

<sup>5</sup> Tomsk State University, pr. Lenina 36, 634050 Tomsk, Russia

<sup>6</sup> St. Petersburg State University, Universitetskaya nab. 7/9, 199034 St. Petersburg, Russia

<sup>7</sup> Universität Augsburg, Institut für Materials Ressource Management, Universitätsstr. 2, 86135 Augsburg, Germany

<sup>8</sup> Faculty of Physics, TU Dresden, 01062 Dresden, Germany

<sup>9</sup> Diamond Light Source, Harwell Campus, Didcot OX11 0DE, United Kingdom

<sup>10</sup> Donostia International Physics Center, Paseo de Manuel Lardizabal 4, 20018 San Sebastian/Donostia, Basque Country, Spain

<sup>11</sup> Departamento de Física de Materiales, Facultad de Ciencias Químicas, and Centro de Física de Materiales and Materials Physics Center, University of the Basque Country (UPV/EHU), 20080 San Sebastian/Donostia, Basque Country, Spain

**Note:** This paper is part of the Special Topic on Topological Semimetals—New Directions.

<sup>a)</sup> Electronic mail: [E.Haubold@ifw-dresden.de](mailto:E.Haubold@ifw-dresden.de)

<sup>b)</sup> Electronic mail: [Florian.Pielhofer@chemie.uni-regensburg.de](mailto:Florian.Pielhofer@chemie.uni-regensburg.de)

<sup>c)</sup> Present address: S. N. Bose National Centre for Basic Sciences, Block-JD, Sector-III, Salt Lake, Kolkata 700106, India.

<sup>d)</sup> Electronic mail: [S.Borisenko@ifw-dresden.de](mailto:S.Borisenko@ifw-dresden.de)

## ABSTRACT

We report experimental and theoretical evidence that GaGeTe is a basic  $Z_2$  topological semimetal with three types of charge carriers: bulk-originated electrons and holes as well as surface state electrons. This electronic situation is qualitatively similar to the classic 3D topological insulator  $\text{Bi}_2\text{Se}_3$ , but important differences account for an unprecedented transport scenario in GaGeTe. High-resolution angle-resolved photoemission spectroscopy combined with advanced band structure calculations show a small indirect energy gap caused by a peculiar band inversion at the  $T$ -point of the Brillouin zone in GaGeTe. An energy overlap of the valence and conduction bands brings both electron and holelike carriers to the Fermi level, while the momentum gap between the corresponding dispersions remains finite. We argue that peculiarities of the electronic spectrum of GaGeTe have a fundamental importance for the physics of topological matter and may boost the material's application potential.

© 2019 Author(s). All article content, except where otherwise noted, is licensed under a Creative Commons Attribution (CC BY) license (<http://creativecommons.org/licenses/by/4.0/>). <https://doi.org/10.1063/1.5124563>

The variety of materials where topology of the electronic structure plays a crucial role in transport properties is rapidly growing.<sup>1–3</sup> The envisioned applications of topological materials in novel devices and quantum information technology will be strongly

influenced by the fine balance between their charge carriers of various types. In classical 3D topological insulators, such as  $\text{Bi}_2\text{Se}_3$ , the transport properties are dictated by the nondegenerate massless topological surface states as well as the electronlike carriers from the

bulk conduction band.<sup>4</sup> In 3D Dirac or Weyl semimetals, the Fermi surface (FS) is formed by single points of band degeneration (type I) or hole and electron pockets touching in discrete points (type II).<sup>3</sup> A bulk material with a comparable number of both types of the bulk charge carriers as well as the spin-momentum locked 2D topological surface states has not yet been accounted for. Such a material would need to have small (semimetallic) Fermi surfaces of both, electron- and holelike character and an inverted, though indirect, bandgap. Here, we put forward GaGeTe as the first example of such conceptually different electronic situation, which we call a basic  $Z_2$  topological semimetal.

The layered compound GaGeTe was synthesized and structurally characterized in 1977<sup>5</sup> and 1983.<sup>6</sup> Its phonon structure,<sup>7</sup> thermoelectric,<sup>8</sup> and transport<sup>9</sup> properties were consequently analyzed. However, the first theoretical study of its bulk electronic structure has only appeared very recently<sup>10</sup> and has sparked strong interest in the surface electronic structure of this material.<sup>11</sup> In Ref. 10, structural and electronic resemblance between a structure fragment of the layered GaGeTe bulk and a heavy analogue of graphene, germanene,<sup>12</sup> has been highlighted. 2D materials with buckled honeycomb atomic arrangements, e.g., silicene, germanene, and stanene, are promising candidates for the realization of new devices. For instance, silicene demonstrates such advantages as high carrier mobility and excellent mechanical flexibility while maintaining compatibility with existing Si-based electronics. Most recent studies establish theoretically<sup>11</sup> and experimentally<sup>13</sup> that

monolayers of GaGeTe, namely, six-atom-thick sheets [Fig. 1(a)] held together by van der Waals bonds, can be exfoliated and are suitable for fabrication of nanodevices including transistors and photodetectors. Ultrathin films of GaGeTe exhibit transport characteristics superior to many other transistors based on 2D-materials, such as high hole mobility and good on/off current ratios.

GaGeTe is not only promising for potential semiconductor applications, but also intriguing from a fundamental perspective. First-principles calculations performed by coauthors in Ref. 10 are highlighting the possibility of a topological band inversion in its electronic spectrum driven by spin-orbit coupling. The valence and conduction bands invert at the  $T$ -point, opening up a narrow indirect gap of the order of 30 meV. The bandgap size appears to be very sensitive to the chosen computational parameters and earlier published experimental studies of the physical properties of GaGeTe neither corroborate nor refute any specific theory result. For instance, an optical study implies that GaGeTe is a semiconductor with the bandgap of 1.12 eV.<sup>9</sup> To shed more light on these ambivalent results of theory and experiment, we have engaged in the present study of high-quality GaGeTe single crystals by synchrotron-based angle-resolved photoemission spectroscopy (ARPES) with variable photon energies. We clarify the details of the electronic structure of GaGeTe and scrutinize its probable topological nature with the aid of state-of-the-art calculations of its bulk and surface electronic structures.

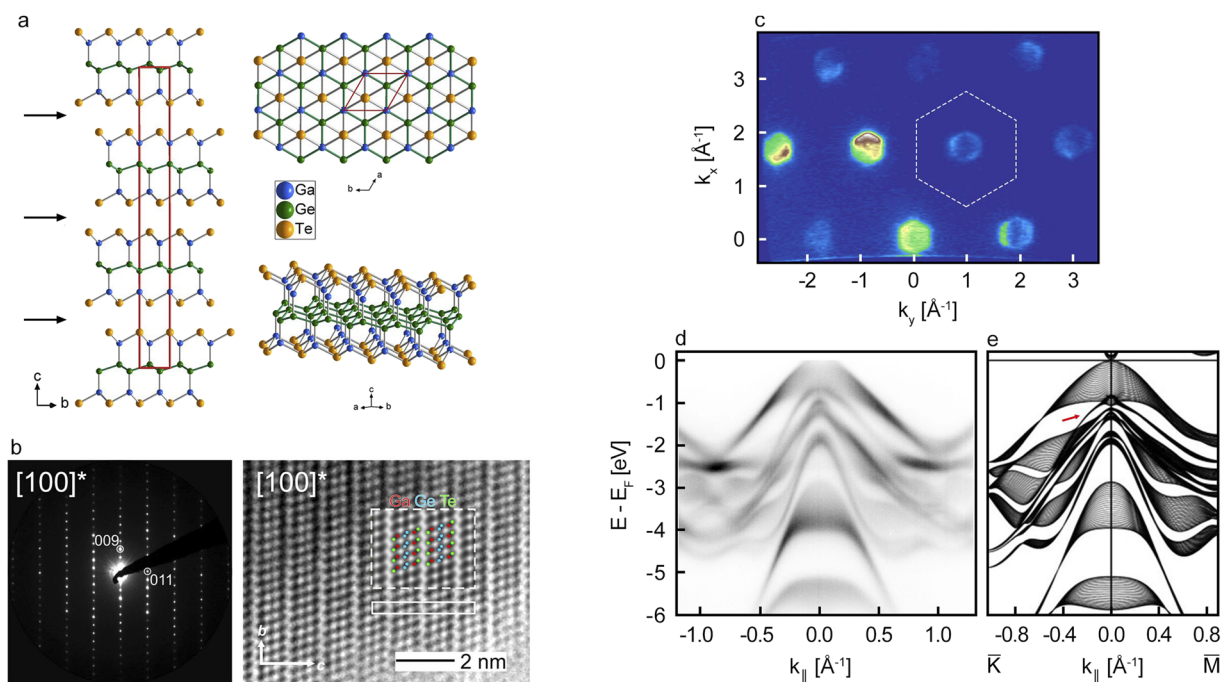


**FIG. 1.** (a) Unit cell of GaGeTe (side and top view) and one sextuple layer, a building unit of the bulk layered structure. The germanenelike buckled Ge-bilayer is highlighted in green. The van der Waals bonded areas are marked by arrows. (b) Main  $[100]^*$  zone PED (left) and experimental  $[100]^*$  zone HRTEM micrograph with simulation ( $\Delta f = -50$  nm,  $t = 4.04$  nm) inset (right). A unit cell is outlined by white solid line. (c) Fermi surface overview map taken at 180 eV. A schematic size of the Brillouin zone is shown with dashed lines. (d) Energy momentum cut taken at 100 eV. (e) Projection of bulk bands onto 2D BZ calculated within DFT. The only major difference to (e) is highlighted by a red arrow.

Single crystals of GaGeTe were obtained following the technique of Ref. 6. It was confirmed experimentally that GaGeTe crystallizes in a trigonal unit cell (sp. gr.  $R\bar{3}m$ ) with an ABC-stacking of sextuple layers [Fig. 1(a)] using the Rietveld refinement (supplementary material, Fig. 2). High-resolution transmission electron microscopy (HRTEM) experiments on selected crystallites reveal ordering along the stacking direction, and precession electron diffraction (PED) patterns accord with the crystal symmetry and lattice parameters found by X-ray diffraction [Fig. 1(b)]. One building unit of GaGeTe [Fig. 1(a)] can be regarded as a corrugated Ge-bilayer (germanene) sandwiched between two [GaTe] sheets of the zinc blende type. Bonding within the sextuple layers is essentially covalent, while the inter-layer interaction is of the van der Waals type. Consequently, the natural cleavage plane of GaGeTe crystals is always Te-terminated, which facilitates the interpretation of the photoemission measurements. Photoemission samples have been cleaved in ultrahigh vacuum, resulting in mirrorlike surfaces allowing us to record, in particular, large Fermi surface (FS) maps. Full experimental details on all methods are given in the supplementary material.

One of such FS maps measured with 180 eV horizontally polarized photons is shown in Fig. 1(c). The FS contour is very small, having the radius of  $0.35 \text{ \AA}^{-1}$ , and it is however larger than that of  $\text{Bi}_2\text{Se}_3$ .<sup>14</sup> The size, shape, and intensity of this contour depend on the momentum and thus imply three-dimensionality of the electronic structure: effective  $k_z$  probed by photons with particular energy is always smaller for larger  $k_x$  and  $k_y$ . For example, the signal is nearly absent for the contour at  $(0 \text{ \AA}^{-1}, 3.5 \text{ \AA}^{-1})$  and its size is smaller for the contour centered at  $(-1.8 \text{ \AA}^{-1}, 0 \text{ \AA}^{-1})$ . Thus, the electron escape depth in this material is sufficient to distinguish between different  $k_z$ 's even using the same photon energy.

We compare the underlying dispersion, experimental and calculated ones, in Figs. 1(d) and 1(e), respectively. As a first step, it is instructive to compare with the  $k_z$ -integrated calculations to find out about the  $k_z$ -resolution mentioned above. Experimental data are taken along the cut running parallel to the  $\bar{K} - \bar{\Gamma} - \bar{M}$  direction of the 2D Brillouin zone (BZ). The projection of the 3D BZ onto the 2D BZ is shown in Fig. 2(a). The overall agreement is remarkable and not only qualitative, especially for the  $\bar{K} - \bar{\Gamma}$  direction: all the dispersion coincide, including the energy positions of the dispersion maxima at zero momentum. The only exception is a two-dimensional band (weak  $k_z$ -dispersion) having a top at  $\sim 0.8 \text{ eV}$  according to the calculations, while the experiment shows the maximum at  $\sim 0.65 \text{ eV}$  binding energy [see the red arrow in Fig. 1(e)]. One can notice that the experiment has more spectral weight at particular  $k_z$  values, although an admixture from other  $k_z$ 's is still visible. This observation agrees well with the moderate  $k_z$ -resolution concluded from the Fermi surface map shown in Fig. 1(c). Within the considered energy range, we note a good agreement between experiment and theory, independent of which exchange-correlation functional, Perdew-Burke-Ernzerhof (PBE) or Heyd-Scuseria-Ernzerhof (HSE), is used to describe the occupied electronic structure of GaGeTe.<sup>10</sup>

We now address the  $k_z$  dependence in more detail by comparing the calculated data at different  $k_z$  positions with the data collected using differing photon energies in Fig. 2. Panels (b)–(e) show a calculated band structure using the PBE functional. The band inversion manifests itself very clearly in the cuts running through the  $T$ -point [Fig. 2(e)]. At other  $k_z$ 's, one can still notice the

characteristic dip in the quickly dispersing holelike band. This trend is confirmed by the experimental data shown in panels (g)–(j). These data were measured using the photon energies from 91 eV (g) to 100 eV (j) in steps of 3 eV. The holelike dispersion is noticeably changing when approaching the Fermi level, highlighted again in panels [(k)–(n)] showing only the topmost 1 eV. In addition to this, one can see that another feature is present at the Fermi level and its intensity is growing together with the intensity of the holelike feature. There is no energy gap visible between them. At higher binding energies, there are bands showing a large  $k_z$  dependency as well, e.g., the bands seen in Figs. 1(d) and 1(e) at  $-1 \text{ eV}$ ,  $-3 \text{ eV}$ , and  $-6 \text{ eV}$  at the  $\Gamma$  point. The corresponding intensity redistribution in the experimental data shown in panels (g)–(j) of Fig. 2 clearly tracks these changes. As expected, the bands with weaker  $k_z$  dispersion are visible in all energy momentum cuts at approximately the same energies.

Summarizing the experimental observations so far, we can conclude that the energy gap is either very small or absent, thus annulling the earlier beliefs that GaGeTe is a semiconductor with a 1.1 eV gap. This, together with the peculiar shape of the dispersion of the holelike band closest to  $E_F$ , clearly speaks in favor of the band inversion and, subsequently, the topological nature of GaGeTe. In this case, topological surface states are expected.

To clarify whether the PBE-based result, and thus the topological band inversion, holds in terms of the gap size, we have carried out typical dosing experiments evaporating potassium on the surface of the sample. The results of these measurements are shown in Fig. 3. The dosing turned out to be effective, and a shift of the chemical potential by nearly half an electron volt [Figs. 3(a) and 3(b)] was achieved. As it was suggested by Figs. 1(d) and 1(e), the top of the holelike band was very close to the Fermi level [Figs. 3(c) and 3(d)]. According to density functional theory (DFT) calculations, in the case of the HSE functional, the band structure is topologically trivial with a rather large direct gap of 550 meV with the gap extrema located exactly in the  $T$ -point of 3D BZ.<sup>10</sup> Our dosing experiments clearly exclude this scenario, as no gap could be observed at all. However, the unlikely scenario of a situation very different from the calculations, where the large gap is would still reside above the dosed chemical potential will be excluded later on.

In accordance with the PBE-based calculations, we have not observed a large energy gap suggested by other functionals including HSE. On the other hand, we also have not observed a small direct energy gap of 30 meV between the valence and conduction bands and a sharp electronlike bottom of the conduction band itself, as suggested by the PBE calculations. Instead, we detected a spectral density at the Fermi level [Fig. 3(d)] with the finite momentum width, which stayed nearly constant and increased only slightly up to the highest dosing level. At higher coverage, the features became too blurred to encourage further dosing. We found out that this intensity could be enhanced using the light of different photon energies, implying that there is indeed not a direct gap between the valence and conduction bands, but an indirect one, ruling out the scenario with a large gap. The electronic structure of GaGeTe is thus characterized by a band inversion, present in an indirect and inverted bandgap, and its nontrivial electronic structure.

We have further analyzed the topological phase in GaGeTe by two methods. At first, the parities of the states at the time-reversal invariant momentum (TRIM) points of the primitive



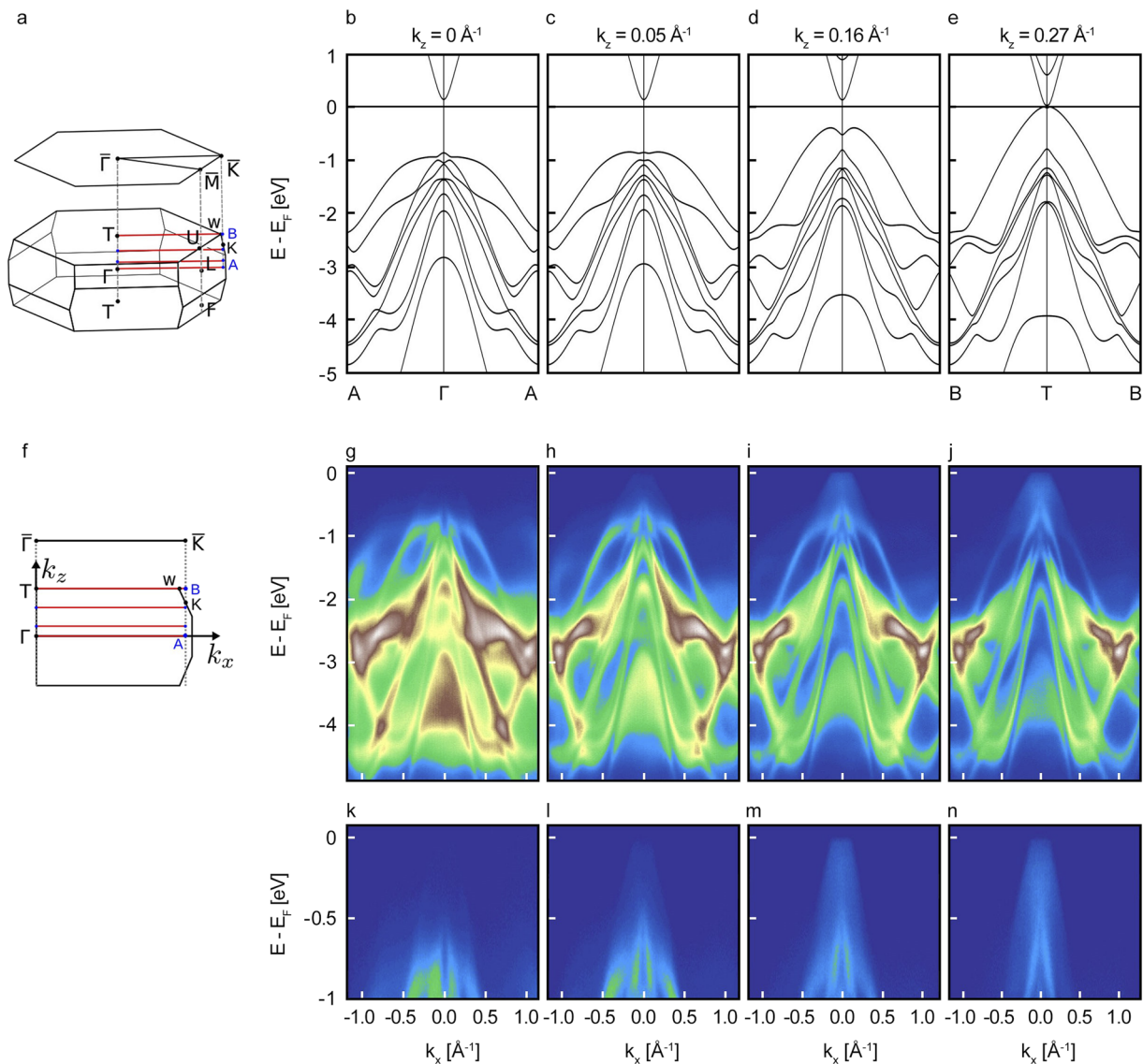


**FIG. 2.** [(a) and (f)] Bulk Brillouin zone with  $k_z$  constant lines (red), along which the electronic spectra were calculated. Above the 3D image in (a) the projected surface is depicted. (b)–(e) calculation corresponding to the electronic band structure in the order of increasing  $k_z$ . (g)–(j) Energy momentum cuts taken with 91 eV–100 eV in equidistant steps. (k)–(n) zoomed-in version of panels (g)–(j) showing the evolution of the topmost band with increasing photon energy.

rhombohedral cell were considered. The results establish a nontrivial character of the electronic structure, as characterized by the topological invariant  $Z_2 = 1; (111)$ , which originates from a bulk band inversion at the  $T$ -point of the 3D Brillouin zone. The edge of the valence zone is constituted by the even states, the  $s$ -orbitals of the Ge atoms, whereas the conduction-band edge is composed of the odd states, the Te  $p$ -orbitals. Away from the region of the band inversion, the orbital composition of the gap edges is reversed. We also checked the topological nature of GaGeTe by varying spin-orbit coupling strength. The gap size decreases down to zero when the spin-orbit coupling strength  $\lambda/\lambda_0$  is diminished to  $\sim 0.65$ , where  $\lambda_0$  is the natural value of the SOC contribution. At smaller  $\lambda/\lambda_0$ , the electronic

spectrum is trivial, the gap edges are not inverted, and  $Z_2$  is equal to 0; (000). Additionally, we also prove the nontrivial topology by the Wilson loop (WL) method proposed in Refs. 15 and 16. It allows us to trace the topology of a material graphically. The WL spectra at  $k_z = 0$  and  $k_z = \pi$  are shown in the [supplementary material](#), Fig. 1. It is evident that the spectra cross an arbitrary reference line an odd number of times at  $k_z = 0.5$  and an even number of times at  $k_z = 0$ . This case corresponds to  $Z_2 = 1; (001)$ . Also at  $\lambda/\lambda_0 < 0.65$ , both for  $k_z = 0$  and  $k_z = \pi$ , the WL bands cross the reference line an even number of times. This finding is also in agreement with the above given analysis of the  $Z_2$  invariant conducted on the basis of the parity of the wave-functions.

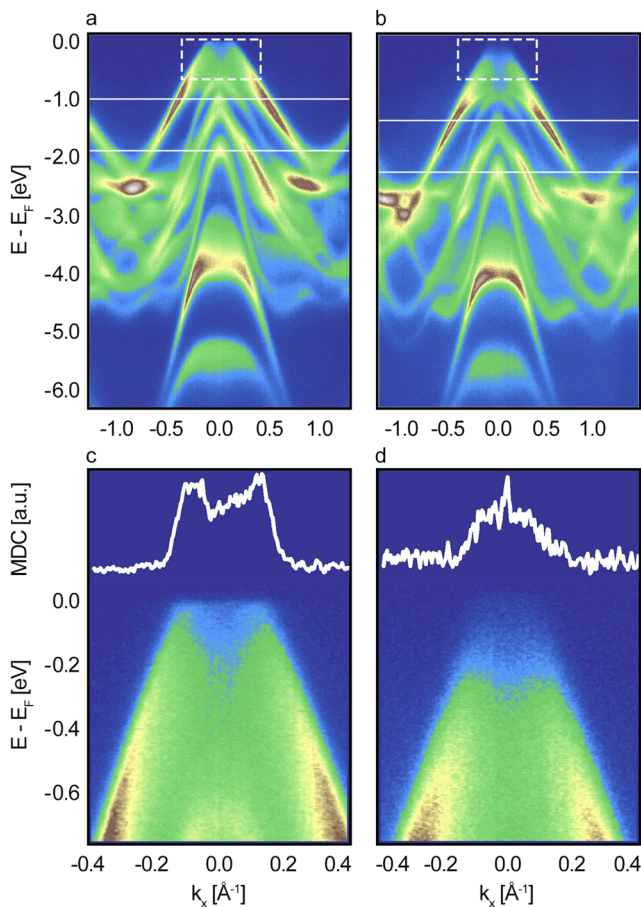


**FIG. 3.** Results of the dosing of single crystals with potassium. (a) Before dosing, (b) After dosing approximately half a monolayer. The center of one distinct band is highlighted with a white line. [(c) and (d)] Zoomed-in pictures close to the Fermi energy, with their respective locations shown with dashed boxes in the respective panels above. The outline of the dispersion is highlighted by a dashed line, and the momentum distribution curve of the Fermi energy is shown above the data.

In Fig. 4, we present the data taken using lower photon energies of 19 eV, to zoom in the region of interest. As we noticed earlier, it is difficult to assign the particular high-symmetry point along the  $\Gamma$ - $T$  pathway to a particular photon energy because of the moderate  $k_z$ -resolution in the case of GaGeTe. In this case, on one hand, the higher intensity of the strongly dispersing holelike band at the higher binding energies (approximately 0.75 eV) would imply this cut corresponds to the vicinity of the  $\Gamma$ -point; on the other hand, the strongest spectral weight at the Fermi level means one is close to the  $T$ -point. In any case, now it is clearly seen that the calculations with the experimental lattice parameters do not reproduce the photoemission experiment in full detail. The most striking observation is that the electronlike dispersion corresponding to the bottom of the conduction band is clearly seen below the Fermi level. We note that this is not a signature of the n-doping since Figs. 1–3 demonstrate that also the valence band crosses the chemical potential. Taking into account the overall agreement with the calculations

on a larger energy scale, we conclude that the deviations preserving a Luttinger count occur. Instead of a semiconductor with a tiny direct gap, experiment shows that GaGeTe is a semimetal with the small bulk-originated Fermi surfaces of both types, a holelike FS, with the shape of a torus due to the crossings of the strongly dispersing holelike band, and an electronlike FS, with the shape of an ellipsoid or even a sphere, supported by the electronlike conduction band with its minimum below the Fermi level near the  $T$ -point [see Fig. 4(a)]. Our calculations demonstrate that the band dispersion in the vicinity of the Fermi energy are extremely sensitive to even minuscule changes in the unit cell parameters and geometry optimization [see Fig. 4, panels (b) and (c)]. For instance, the described experimental picture can be qualitatively confirmed computationally with a slightly extended unit cell parameter  $a$ , namely, from 4.08  $\text{\AA}$  to 4.13  $\text{\AA}$ . To keep the cell volume constant, the lattice parameter  $c$  has been contracted from 34.54  $\text{\AA}$  to 33.90  $\text{\AA}$ . In both cases, the material is topological and qualitatively similar surface states should be present, as seen in panels (c) and (d). We identify those as straight linear dispersion accompanying the conduction band states down to approximately 0.6 eV in the experimental spectra shown in panel (e). Second derivative [panel (f)] helps to distinguish them from the bulk projections of the valence and conduction bands. Therefore, the experimental gap, observed by us, is simultaneously indirect and inverted and this can be accounted by the calculations with slightly strained lattice.

Although the situation in GaGeTe is qualitatively similar to the simplest 3D topological insulator  $\text{Bi}_2\text{Se}_3$ , there are important differences. First is that GaGeTe does not have a direct gap and is a semimetal in contrast to  $\text{Bi}_2\text{Se}_3$ ,<sup>17</sup> i.e., the valence and conduction bands overlap in energy and both cross the Fermi level resulting in small Fermi surfaces. Second, the sizes of an energy gap at a particular  $k$ -point and of a momentum gap at particular energy are much smaller: less than 200 meV and less than 0.1  $\text{\AA}^{-1}$ , respectively, which is in agreement with the calculations shown in Fig. 4. The surface states themselves are less robust than in  $\text{Bi}_2\text{Se}_3$ . This is related to the quality of the surface after the cleavage of the sample in ultrahigh vacuum. Despite the layered structure of GaGeTe, it is very difficult to obtain a relatively big shiny portion of the atomically clean surface. In such cases, the surface states are known to be elusive and require repeating experiments to be detected. One of such successful attempts is documented in Fig. 4. The surface states support another small Fermi surface, which we schematically depict in panel (a) as a cylinder together with the bulk originated 3D Fermi surfaces. Our calculations show that these topological surface states are spin-polarized.

The bulk GaGeTe thus emerges as a basic  $Z_2$  topological semimetal. There is only one Dirac cone formed by the topological surface states per Brillouin zone. Unlike the similar electronic structure of Sb-Bi-Sb heterostructures,<sup>18,19</sup> the number of bulk charge carriers of the opposite types is the same in GaGeTe. As previous studies<sup>10,11,13</sup> and this study have demonstrated, the electronic structure of GaGeTe is very sensitive to a number of parameters and therefore is very attractive for nanodevice fabrication. It can be tuned by strain, exfoliation, doping, and gating. GaGeTe is stable on air and not moisture-sensitive. At the same time, the monolayer of GaGeTe seems to be dynamically and thermodynamically stable at very high temperatures.<sup>11</sup> Having such a peculiar Fermi surface [Fig. 4(a)] with two 3D sheets and one 2D sheet, the hypothetical shift of the

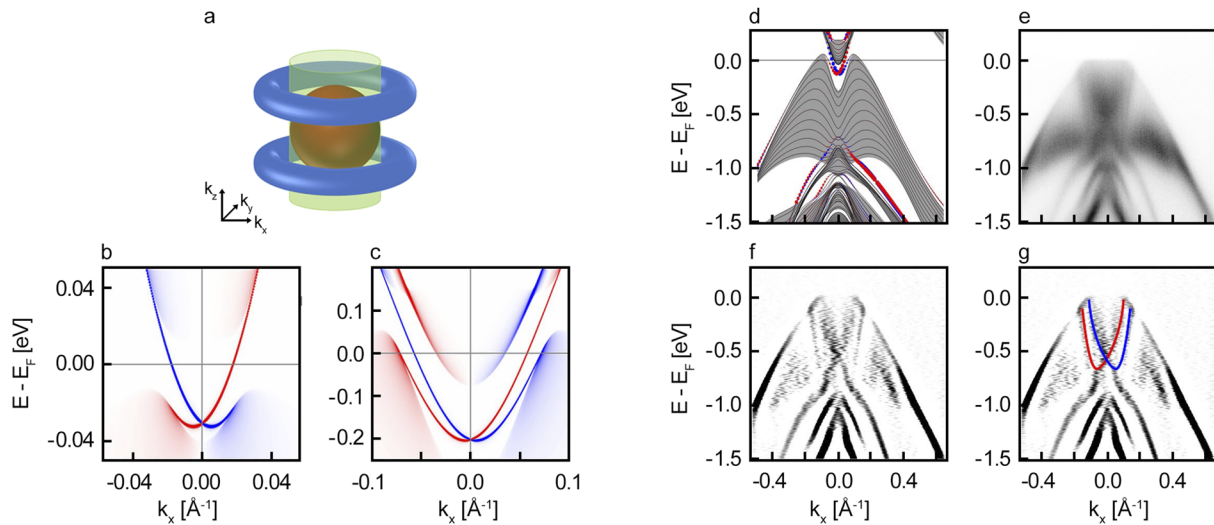


**FIG. 4.** (a) Schematic of the Fermi surface with an electron pocket (red), hole pockets (blue), and surface states (green). [(b) and (c)] Spin-resolved surface spectral function calculated within *ab initio* based tight binding model with the experimentally determined unit cell parameters (b) and with the unit cell parameter *a* expanded by 1% (c). Spin-polarization is color-coded (red and blue). Spectrum (b) shows the initially expected direct bandgap, whereas spectrum [(c) and (d)] highlight an indirect bandgap actually found by photoemission experiments. (e) 19 eV energy momentum cut taken at the T-point. (f) 2nd derivative of (e), highlighting the edges in panel (d). (g) same as (f), but with the dispersions identified as surface states marked in red and blue.

Fermi level can switch the system from having purely bulk n-type charge carriers to having purely p-type ones. In between these two extremes, the presence of the nondegenerate topological surface states with the spin-texture can be exploited.

Besides GaGeTe, there are a few other materials that may be nominally categorized as a  $Z_2$  topological semimetal. The natural superlattice phase Bi<sub>4</sub>Se<sub>3</sub>, the low temperature form of Au<sub>2</sub>Pb,<sup>20</sup> the rare earth monpnictides LaSb<sup>21</sup> and LaBi,<sup>22–25</sup> and elemental Sb show a momentum gap, semimetallic electronic spectra and a topological band inversion in the 3D BZ based on band structure calculations. Only Bi<sub>4</sub>Se<sub>3</sub>,<sup>26</sup> LaBi,<sup>27</sup> and elemental Sb<sup>28</sup> have been experimentally confirmed to host topological surface states. In the case of LaSb, the prediction of a  $Z_2$  topological phase or trivial phase depends on the applied DFT functional.<sup>21</sup> Although experimental verification via ARPES was probed several times,<sup>27,29</sup> it is unclear whether the observed Dirac like surface state of this material makes it a topological nontrivial material or not, since it is not possible to state if the number of band inversions is odd or even.<sup>27</sup> Heterostructures of both LaSb and LaBi are further predicted to be topologically nontrivial.<sup>21</sup> A HgTe/HgCdTe quantum well<sup>30</sup> can be regarded as a 2D analog of GaGeTe.

Characterizing the electronic structure, even via a combination of ARPES and band structure calculations, can be a real issue as represented by the case of ZrTe<sub>5</sub>. It was heavily discussed what kind of nontrivial topology can be deduced from the electronic spectrum, since the electronic band structure of this material is extremely sensitive to strain and undergoes a phase transition from a strong to a weak topological insulator via a Dirac semimetal state.<sup>31–34</sup>

The ARPES measurements of GaGeTe presented here clarify the contradicting theoretical predictions previously reported in Ref. 10. GaGeTe as a  $Z_2$  topological semimetal may have a

fundamental importance for the physics of topological matter as peculiar transport characteristics in the proximity of a topological transition greatly boost the application potential in fields of electronics or energy harvesting. Its 2D nature allows for exfoliation and makes it very attractive for thin film growth and device fabrication. With ARPES, the band structure was measured and the evolution of the topmost bands was tracked along the  $k_z$  direction. Together with the exclusion of a large band gap using potassium doping, the PBE functional was identified to be more accurate than the HSE hybrid functional. These results indicate the topological nature of this compound, supported by topological features revealed with ARPES. The example of GaGeTe demonstrates the complexity of precise predictions based on band structure calculations and the need of experimental confirmation.

See the [supplementary material](#) for details about the experimental methods used as well as calculation details.

This work was supported by DFG under the Grant No. BO 1912/7-1 as well as Grant Nos. IS 250/2-1 and PF 324/4-1 of the SPP 1666 program, Grant No. RU 776/15-1 of the ERANET-Chemistry program, Tomsk State University Project No. 8.1.01.2018, and St. Petersburg University Project No. 15.61.202.2015. Calculations were performed at the SKIF-Cyberia supercomputer of Tomsk State University and supported by RSF, grant No. 18-12-00169. The authors acknowledge Diamond Light Source for the beamtime at I05 beamline under Proposal No. SI18586 as well as the BESSY II Berlin for the beamtime at I<sup>3</sup> ARPES station under Proposal Nos. 171-05051CR and 172-05659CR/R. The research leading to this result has been supported by the project CALIPSOplus under the Grant Agreement No. 730872 from the EU Framework Programme for Research and Innovation HORIZON 2020. S.B. is grateful to



BMW Germany for the support within the framework of WIPANO program (Grant No. N 03THW12H04). S.B. is also grateful to BMBF Germany for the support within the framework of Ukrainian-German Excellence Center UKRATOP project.

## REFERENCES

- <sup>1</sup>Y. Ando, "Topological insulator materials," *J. Phys. Soc. Jpn.* **82**, 102001 (2013).
- <sup>2</sup>Y. Ando and L. Fu, "Topological crystalline insulators and topological superconductors: From concepts to materials," *Annu. Rev. Condens. Matter Phys.* **6**, 361–381 (2015).
- <sup>3</sup>N. P. Armitage, E. J. Mele, and A. Vishwanath, "Weyl and Dirac semimetals in three-dimensional solids," *Rev. Mod. Phys.* **90**, 015001 (2018).
- <sup>4</sup>M. Z. Hasan and C. L. Kane, "Colloquium: Topological insulators," *Rev. Mod. Phys.* **82**, 3045–3067 (2010).
- <sup>5</sup>G. Kra, R. Eholie, and J. Flahant, *C. R. Seances Acad. Sci., Ser. C* **284**, 889–892 (1977).
- <sup>6</sup>D. Fenske and H. G. V. Schnering, "GaGeTe, eine neue defekt-tetraederstruktur," *Angew. Chem.* **95**, 420–421 (1983).
- <sup>7</sup>E. López-Cruz, M. Cardona, and E. Martínez, "Raman spectrum and lattice dynamics of GaGeTe," *Phys. Rev. B* **29**, 5774–5777 (1984).
- <sup>8</sup>V. Drašar, V. Kucek, L. Beneš, and P. Lošták, "Thermoelectric properties and nonstoichiometry of GaGeTe," *AIP Conf. Proc.* **1449**, 267–270 (2012).
- <sup>9</sup>V. Kucek, C. Drasar, J. Navratil, L. Benes, and P. Lostak, "Optical and transport properties of GaGeTe single crystals," *J. Cryst. Growth* **380**, 72–77 (2013).
- <sup>10</sup>F. Pielnhofer, T. V. Menshchikova, I. P. Rusinov, A. Zeugner, I. Yu. Sklyadnaya, R. Heid, K.-P. Bohnen, P. Golub, A. I. Baranov, E. V. Chulkov, A. Pfizner, M. Ruck, and A. Isaeva, "Designing 3D topological insulators by 2D-Xene (X = Ge, Sn) sheet functionalization in GaGeTe-type structures," *J. Mater. Chem. C* **5**, 4752–4762 (2017).
- <sup>11</sup>J. Zhang, S.-s. Li, W.-x. Ji, C.-w. Zhang, P. Li, S.-f. Zhang, P.-j. Wang, and S.-s. Yan, "Two-dimensional GaGeTe film: A promising graphene-like material with tunable band structure and high carrier mobility," *J. Mater. Chem. C* **5**, 8847–8853 (2017).
- <sup>12</sup>M. E. Dávila, L. Xian, S. Cahangirov, A. Rubio, and G. L. Lay, "Germanene: A novel two-dimensional germanium allotrope akin to graphene and silicene," *New J. Phys.* **16**, 095002 (2014).
- <sup>13</sup>W. Wang, L. Li, Z. Zhang, J. Yang, D. Tang, and T. Zhai, "Ultrathin GaGeTe p-type transistors," *Appl. Phys. Lett.* **111**, 203504 (2017).
- <sup>14</sup>A. A. Kordyuk, T. K. Kim, V. B. Zabolotnyy, D. V. Evtushinsky, M. Bauch, C. Hess, B. Büchner, H. Berger, and S. V. Borisenko, "Photoemission-induced gating of topological insulators," *Phys. Rev. B* **83**, 081303 (2011).
- <sup>15</sup>A. A. Soluyanov and D. Vanderbilt, "Wannier representation of  $z_2$  topological insulators," *Phys. Rev. B* **83**, 035108 (2011).
- <sup>16</sup>R. Yu, X. L. Qi, A. Bernevig, Z. Fang, and X. Dai, "Equivalent expression of  $z_2$  topological invariant for band insulators using the non-Abelian Berry connection," *Phys. Rev. B* **84**, 075119 (2011).
- <sup>17</sup>I. A. Nechaev, R. C. Hatch, M. Bianchi, D. Guan, C. Friedrich, I. Aguilera, J. L. Mi, B. B. Iversen, S. Blügel, P. Hofmann, and E. V. Chulkov, "Evidence for a direct band gap in the topological insulator Bi<sub>2</sub>Se<sub>3</sub> from theory and experiment," *Phys. Rev. B* **87**, 121111 (2013).
- <sup>18</sup>A. Takayama, T. Sato, S. Souma, and T. Takahashi, "Rashba effect in antimony and bismuth studied by spin-resolved ARPES," *New J. Phys.* **16**, 055004 (2014).
- <sup>19</sup>G. Bihlmayer, Y. M. Koroteev, E. V. Chulkov, and S. Blügel, "Surface- and edge-states in ultrathin Bi-Sb films," *New J. Phys.* **12**, 065006 (2010).
- <sup>20</sup>L. M. Schoop, L. S. Xie, R. Chen, Q. D. Gibson, S. H. Lapidus, I. Kimchi, M. Hirschberger, N. Haldolaarachchige, M. N. Ali, C. A. Belvin, T. Liang, J. B. Neaton, N. P. Ong, A. Vishwanath, and R. J. Cava, "Dirac metal to topological metal transition at a structural phase change in Au<sub>2</sub>Pb and prediction of  $z_2$  topology for the superconductor," *Phys. Rev. B* **91**, 214517 (2015).
- <sup>21</sup>U. Dey, M. Chakraborty, A. Taraphder, and S. Tewari, "Bulk band inversion and surface Dirac cones in LaSb and LaBi: Prediction of a new topological heterostructure," *Sci. Rep.* **8**, 14867 (2018).
- <sup>22</sup>P.-J. Guo, H.-C. Yang, B.-J. Zhang, K. Liu, and Z.-Y. Lu, "Charge compensation in extremely large magnetoresistance materials LaSb and LaBi revealed by first-principles calculations," *Phys. Rev. B* **93**, 235142 (2016).
- <sup>23</sup>J. Nayak, S.-C. Wu, N. Kumar, C. Shekhar, S. Singh, J. Fink, E. E. Rienks, G. H. Fecher, S. S. Parkin, B. Yan *et al.*, "Multiple Dirac cones at the surface of the topological metal LaBi," *Nat. Commun.* **8**, 13942 (2017).
- <sup>24</sup>R. Lou, B.-B. Fu, Q. Xu, P.-J. Guo, L.-Y. Kong, L.-K. Zeng, J.-Z. Ma, P. Richard, C. Fang, Y.-B. Huang *et al.*, "Evidence of topological insulator state in the semimetal LaBi," *Phys. Rev. B* **95**, 115140 (2017).
- <sup>25</sup>U. Dey, "Comparative study of the compensated semi-metals LaBi and LuBi: A first-principles approach," *J. Phys.: Condens. Matter* **30**, 205501 (2018).
- <sup>26</sup>Q. Gibson, L. M. Schoop, A. Weber, H. Ji, S. Nadj-Perge, I. Drozdov, H. Beidenkopf, J. Sadowski, A. Fedorov, A. Yazdani *et al.*, "Termination-dependent topological surface states of the natural superlattice phase Bi<sub>2</sub>Se<sub>3</sub>," *Phys. Rev. B* **88**, 081108 (2013).
- <sup>27</sup>X. Niu, D. Xu, Y. Bai, Q. Song, X. Shen, B. Xie, Z. Sun, Y. Huang, D. Peets, and D. Feng, "Presence of exotic electronic surface states in LaBi and LaSb," *Phys. Rev. B* **94**, 165163 (2016).
- <sup>28</sup>D. Hsieh, L. Wray, D. Qian, Y. Xia, J. Dil, F. Meier, L. Patthey, J. Osterwalder, G. Bihlmayer, Y. Hor *et al.*, "Direct observation of spin-polarized surface states in the parent compound of a topological insulator using spin- and angle-resolved photoemission spectroscopy in a Mott-polarimetry mode," *New J. Phys.* **12**, 125001 (2010).
- <sup>29</sup>H. Oinuma, S. Souma, D. Takane, T. Nakamura, K. Nakayama, T. Mitsuhashi, K. Horiba, H. Kumigashira, M. Yoshida, A. Ochiai *et al.*, "Three-dimensional band structure of LaSb and CeSb: Absence of band inversion," *Phys. Rev. B* **96**, 041120 (2017).
- <sup>30</sup>S. V. Gudina, A. S. Bogolyubskii, V. N. Neverov, N. G. Shelushinina, and M. V. Yakunin, "Extremum loop" model for the valence-band spectrum of a HgTe/HgCdTe quantum well with an inverted band structure in the semimetallic phase," *Semiconductors* **52**, 1403–1406 (2018).
- <sup>31</sup>X.-B. Li, W.-K. Huang, Y.-Y. Lv, K.-W. Zhang, C.-L. Yang, B.-B. Zhang, Y. Chen, S.-H. Yao, J. Zhou, M.-H. Lu *et al.*, "Experimental observation of topological edge states at the surface step edge of the topological insulator ZrTe<sub>5</sub>," *Phys. Rev. Lett.* **116**, 176803 (2016).
- <sup>32</sup>R. Chen, S. Zhang, J. Schneeloch, C. Zhang, Q. Li, G. Gu, and N. Wang, "Optical spectroscopy study of the three-dimensional Dirac semimetal ZrTe<sub>5</sub>," *Phys. Rev. B* **92**, 075107 (2015).
- <sup>33</sup>R. Chen, Z. Chen, X.-Y. Song, J. Schneeloch, G. Gu, F. Wang, and N. Wang, "Magnetoinfrared spectroscopy of Landau levels and Zeeman splitting of three-dimensional massless Dirac fermions in ZrTe<sub>5</sub>," *Phys. Rev. Lett.* **115**, 176404 (2015).
- <sup>34</sup>Z. Fan, Q.-F. Liang, Y. Chen, S.-H. Yao, and J. Zhou, "Transition between strong and weak topological insulator in ZrTe<sub>5</sub> and HfTe<sub>5</sub>," *Sci. Rep.* **7**, 45667 (2017).